The International Journal of Advanced Manufacturing Technology (2019) 105:4899–4907
https://doi.org/10.1007/s00170-019-04072-8

ORIGINAL ARTICLE

Cell patterning via optimized dielectrophoretic force within hexagonal electrodes in vitro for skin tissue engineering

Zhijie Huan[1] · Weicheng Ma[1] · Min Xu[1] · Zhixiong Zhong[2] · Xiangpeng Li[3] · Zhenhong Zhu[4]

Received: 5 March 2019 / Accepted: 21 June 2019 / Published online: 20 July 2019

Abstract
Tissue reconstruction through in vitro cell seeding is a popular method for tissue engineering. In this paper, we proposed a thin-layer structure consisting of multiple hexagons for the regeneration of skin tissue. Cells could be seeded and cultured within the structure via dielectrophoresis (DEP) actively. A thin layer of the structure was fabricated with biocompatible medical-grade stainless steel via precise laser cutting. The fabricated layers were stacked together to form a 3D electrode pair, which could be used to generate a 3D electric field. Thus, the suspended cells within the structure could be patterned via DEP manipulation. The input voltage was examined and optimized to ensure cell viability and patterning efficiency during the DEP manipulation process. As soon as we applied the optimized voltage, human foreskin fibroblast (HFF) cells could be attracted along the edge of the electrodes, forming hexagonal cellular patterns. After that, a single layer of the patterned cells was further cultured in an incubator for 7 days and observed under a microscope. The obtained images showed that the seeded cells could proliferate and fill in the hexagonal wells, which could be used for further skin tissue regeneration. As shown in the experimental results, this structure could be used for active cell seeding and proliferation for the development of skin tissue engineering.

Keywords Optimized DEP force · Active cell patterning · Novel scaffold · Cell proliferation

1 Introduction

Artificial skin plays an important role in wound healing for severely burned patients. One common way to construct skin tissue in vitro is to seed sufficient cells onto a scaffold. The scaffold is utilized as a physical support guiding cells to proliferate into the skin tissue. In recent decades, numerous researchers have studied the construction of various scaffolds for cell adhesion and growth. Andrés et al. presented the in vitro assessment of a porous polydimethylsiloxane (PDMS) scaffold for hMSC culturing. The scaffold prototypes served as a 3D platform for cell adhesion and growth [1]. Vashisth et al. introduced novel gellan-polyvinyl alcohol (PVA) nanofibers as biodegradable scaffolds for culturing human dermal fibroblast cells [2]. Sadeghi-Avalshahr et al. investigated a mixture of poly(lactic-co-glycolic acid) (PLGA) and collagen to construct a composite scaffold for skin substitute application [3]. PLGA could provide good mechanical properties, and collagen improves the interaction of the seeded cells. Zhang et al. combined a biodegradable and biocompatible poly(glycerol sebacate) material with silk fibroin microfibers and chitosan and fabricated a porous scaffold for dermal skin substitutes [4]. Oliveira et al. reported a 3D scaffold made of bioactive glass powders using 3D printing, which has the potential for bone tissue regeneration [5].

However, conventional cell-seeding processes in skin tissue engineering are usually passive and time-consuming with a sufficient number of cells suspended in the medium [6]. Moreover, the obtained cellular pattern is uncontrollable due to the uneven distribution of target cells. Because the population of autologous cells from severely burned patients is scarce, improving the efficiency of the cell-seeding process

✉ Zhijie Huan
hzjxb@mail.ustc.edu.cn

[1] School of Electrical Engineering and Automation, XiaMen University of Technology, No. 600 Ligong Road, Jimei District, Xiamen 361024, Fujian, China

[2] Fujian Provincial Key Laboratory of Information Processing and Intelligent Control, MinJiang University, Fuzhou, Fujian, China

[3] College of Mechanical and Electrical Engineering, Soochow University, Suzhou, Jiangsu, China

[4] Children's Hospital of Soochow University, Suzhou, Jiangsu, China

is necessary. Therefore, we combined the DEP mechanism with a porous scaffold to enhance the cell-patterning efficiency and provide a substrate for cell adhesion and proliferation.

The DEP force has been widely studied for cell manipulation due to its non-invasiveness. Compared with other non-invasive techniques, such as optical tweezers [7–11], acoustics [12, 13], and magnetic fields [14–16], DEP is relatively more effective for separating and manipulating groups of cells without any other modification in tissue engineering. Alazzam et al. reported an interdigitated comb-like electrode for the continuous separation of cancer cells from blood via DEP [17]. Ho et al. designed a lobule-mimetic chip for liver-cell patterning that could be used for on-chip reconstruction of liver tissue in vitro [18].

In this paper, we proposed a thin-layer structure consisting of multiple hexagons for the regeneration of skin tissue. Cells could be seeded and cultured within the structure via dielectrophoresis (DEP) in three dimensions actively. Experiments were conducted to verify the optimization of the input voltage to ensure the cell viability and patterning efficiency during the manipulation process. As observed under the microscope, both the bright-field micro-image and fluorescence image showed that the cellular patterns integrated along the proposed electrodes. After the DEP manipulation, the thin layer of cellular pattern was separated and further cultured. The results showed that the patterned cells could proliferate and fill in the hexagonal wells within the structure. Therefore, the proposed structure and voltage input strategy could be used for the patterning of mammalian cells and for the further development of skin tissue regeneration.

2 Materials and methods

2.1 DEP mechanism

The dielectrophoresis effect was first proposed by Pohl [19]. Dielectrophoretic force is a non-invasive method that can be used for cell manipulation. A cell that is placed in a non-uniform electric field will be polarized. The applied electric field induces a dipole in the cell, and an electric force will be generated on each side of the cell. Because the electric field is non-uniform, a net force drives the cell to move along the electric field gradient. The DEP force induced on a spherical cell suspended in a certain solution is given by [20]:

$$F_{DEP} = 2\pi\varepsilon_s R^3 Re[K(\omega)]\nabla E_{rms}^2 \tag{2.1}$$

where ε_s is the relative permittivity of the solution, R is the spherical radius of the suspended cell, and E_{rms} is the root mean square of the electric field strength. $Re[K(\omega)]$ is the real part of the Clausius-Mossotti (CM) factor, given by:

$$K(\omega) = \frac{\varepsilon_c^* - \varepsilon_s^*}{\varepsilon_c^* + 2\varepsilon_s^*}, \varepsilon_c^* = \varepsilon_c - j\frac{\sigma_c}{\omega}, \text{and } \varepsilon_s^* = \varepsilon_s - j\frac{\sigma_s}{\omega} \tag{2.2}$$

where σ_s is the conductivity of the solution, ε_c and σ_c are the permittivity and conductivity of the suspended cell, respectively, and ω is the frequency of the input voltage.

As presented in Eq. (2.2), $Re[K(\omega)]$ varies with the frequency of the applied AC voltage. Moreover, the value of $Re[K(\omega)]$ depends on whether the cell is more or less polarizable than the solution. The direction of the DEP force depends on the sign of $Re[K(\omega)]$. If $Re[K(\omega)] > 0$, the cells will be manipulated by positive dielectrophoresis (p-DEP) and attracted to the regions of highest field strength, as shown in Fig. 1a. In contrast, the cells will be repelled from these regions by negative dielectrophoresis force [21], as shown in Fig. 1b. Therefore, with the construction of certain electrode structures, we can create an electric field for manipulating cells into desired cellular patterns.

2.2 DEP manipulation scaffold design and fabrication

To enhance the patterning efficiency, the DEP mechanism was introduced for the invasive manipulation of cells. A pair of electrodes should be used to generate the non-uniform electric field so that the DEP net force could be induced on the polarized cells.

As shown in Fig. 2, a multi-layer structure was designed to be the manipulator and container. The conductive layers were fabricated with medical-grade stainless steel with a thickness of 200 μm using precise laser cutting. Medical-grade stainless steel exhibits relatively high conductivity and biocompatibility [22]. To avoid short-circuiting within these electrodes, thin layers of polydimethylsiloxane (PDMS) were sandwiched between adjusted conductive layers, as illustrated in the separated layers of the structure in Fig. 2b. PDMS is one of the most commonly used silicon-based polymers in biomedical engineering with excellent biocompatibility and could be used for cell culturing [23, 24].

Moreover, on the top and bottom of the structure, layers of PDMS with a thickness of 2 mm were attached, forming a chamber to hold the cell medium, as shown in Fig. 2b. As we stacked the separated layers together with a plasma bonding machine, micro-wells could be formed within the structure shown in Fig. 2c, which could be utilized for cell manipulation. The whole structure was bonded onto a 35-mm culture petri dish.

We used the process presented in Fig. 3 to seed randomly distributed cells along the fabricated hexagonal structure utilizing a positive DEP force. After patterning the cells, we removed the voltage and replaced the medium with cell culture medium. The whole seeded structure was then placed into an incubator to enhance cell proliferation. After days of

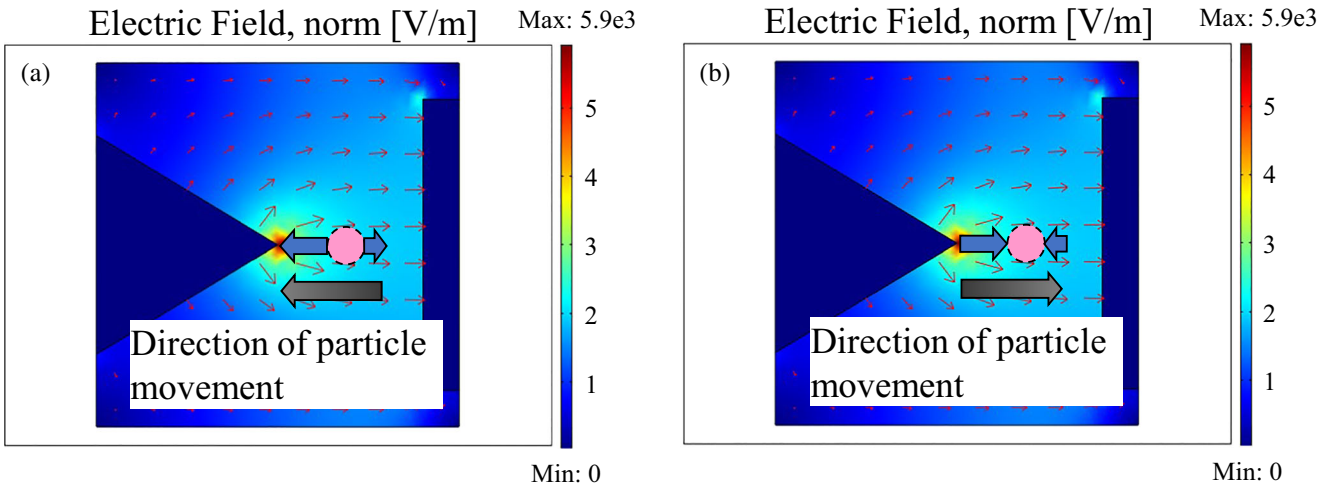

Fig. 1 Numerical simulation for positive DEP manipulation (**a**) and negative DEP manipulation (**b**)

culturing, the patterned cells may stretch and fill in the space of the hexagonal structure so that the cells could further form a thin layer of skin tissue.

2.3 Entire experimental setup for cell patterning

Because the cell-patterning process was driven by dielectrophoresis, an AC function generator (AFG2225, GW Instek) was connected onto the electrodes of the proposed structure with a frequency range of 0.5 Hz~5 MHz and a voltage range of 0~10 V. The stacked scaffold was bonded onto a cell culture petri dish to hold the cell-suspending medium during the patterning experiment, which could further provide a vessel for cell culturing. Prior to the patterning experiments, the whole structure was immersed in a 70% ethanol solution to sterilize the surface of the electrodes. Then, poly-L-lysine was coated, which could be used to promote cell adhesion to solid substrates [25].

To observe the cell-patterning process in real time, an inverted microscope from Nikon (Eclipse Ti) was connected to a digital CCD camera. Thus, the experimental results could be displayed on a computer. The whole petri dish was placed on the heated stage of the microscope system, which could maintain the structure at 37 °C so that we could reduce the cell mortality rate during the manipulation process. Figure 4 presents the entire DEP manipulation system, which was set on a vibration isolation platform to reduce the influence of the surroundings.

2.4 Preparation of cells

In the manipulation experiment, human foreskin fibroblast (HFF) cell lines were used to evaluate the efficiency of the proposed structure. The HFF cells were divided from neonatal human foreskin. The isolated cells were maintained in mixed culture medium in a petri dish containing Dulbecco's modified Eagle's medium (DMEM) with 10% (v/v) heat-

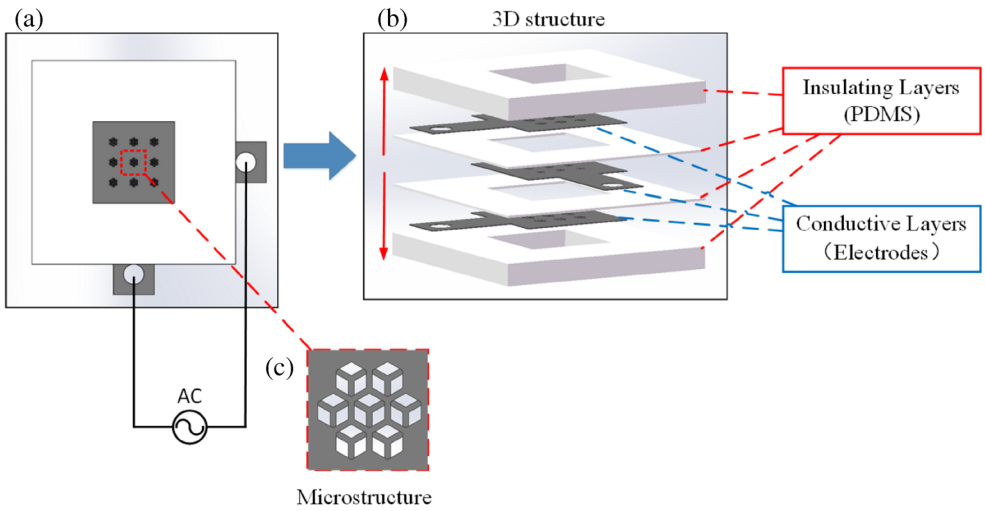

Fig. 2 Schematic of the designed structure for cell manipulation

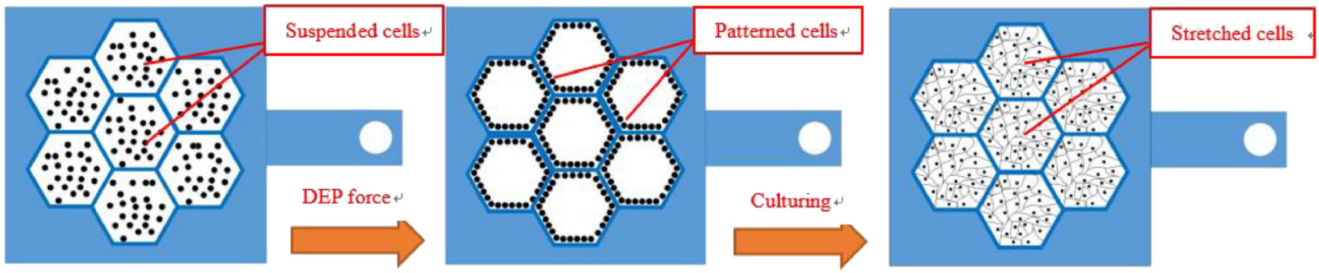

Fig. 3 Schematic of the patterning and culturing process within the hexagonal electrode chips via dielectrophoresis

inactivated fetal bovine serum (FBS) and 1% (v/v) penicillin. For further propagation, the cellular medium was maintained in an incubator at 37 °C and a relative humidity of 95% with 5% CO_2. The culture medium should be replaced every 2 days.

The HFF cells were detached from the petri dish in a laminar flow cabinet prior to the experiment. The cell culture medium was pipetted from the dish, and phosphate-buffered saline (PBS) was utilized to wash away the residual medium. After that, we used a 0.25% trypsin–EDTA solution to detach the HFF cells and transferred the solution to a centrifuge tube. A centrifuge was used to isolate the cell lines. Finally, the culture medium was replaced by a DEP buffer medium with low conductivity, containing 8.5% sucrose, 0.3% dextrose, and 20 mg/L $CaCl_2$, which guaranteed that a positive DEP force could be induced on the polarized cells. The cell concentration of the medium was adjusted to be 1.2×10^6 cells/mL for DEP patterning.

2.5 Cell viability testing

The viability of the HFF cells manipulated with different voltage parameters was collected from the structure. The collected cell medium was added with a 0.4% trypan blue solution, which is routinely used as a cell stain to assess cell viability in dye exclusion tests. Live cells with intact cell membranes will not be colored since the cells are very selective in the compounds that pass through the membrane; in a viable cell, trypan blue is not absorbed. However, dead cells appear as a distinctive blue color under a microscope. The mixed solution was maintained in an incubator for 10 min. After that, a droplet of the medium was pipetted onto a glass slide and observed under a microscope. A hemocytometer was utilized for counting the viable cells within the test quickly and accurately to calculate the cell viability.

3 Results and discussion

3.1 Optimization of input voltage

During the manipulation, the entire scaffold was immersed in DEP buffer medium in a 35 petri dish. As displayed in Fig. 5, during the manipulation, the suspended cell would be driven under a net force, which contains the positive DEP force, gravity, buoyancy, and the viscous drag. The moving direction and speed are determined by the induced net force. The positive DEP force is induced as soon as we applied the voltage, as was given in Eq. (2.1). Since the HFF cells we used in the experiments have a greater density than that of the medium, gravity F_{Grav} is much larger than buoyancy F_{Buoy}. According to Stoke's theorem [26], the cell should overcome the drag force F_{Drag} induced by the medium, which is opposite to the direction of cell movement. The mentioned forces are given as:

$$F_{Grav} = \frac{4}{3}\pi R^3 \rho_c g \tag{3.1}$$

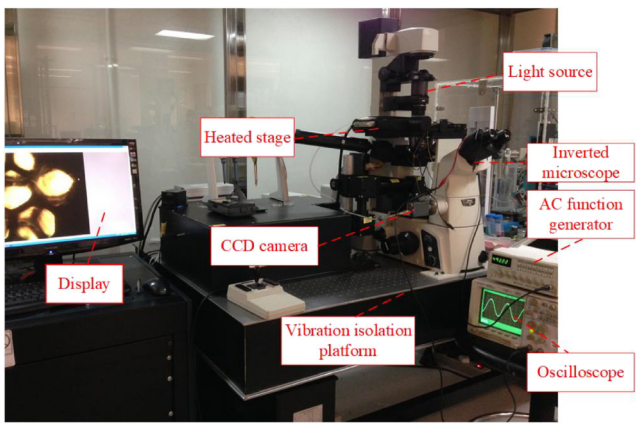

Fig. 4 Entire experimental system for cell manipulation

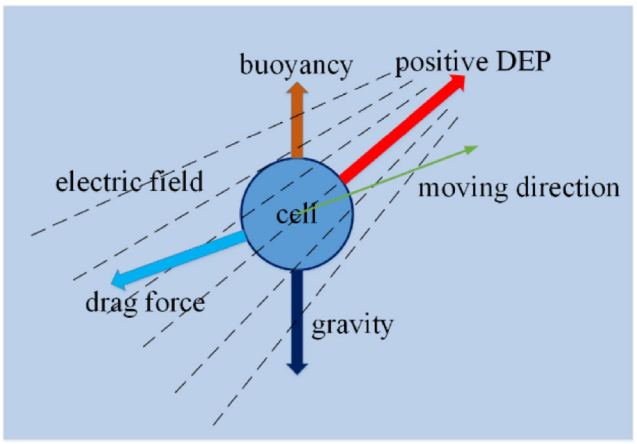

Fig. 5 Force body diagram for a suspended cell

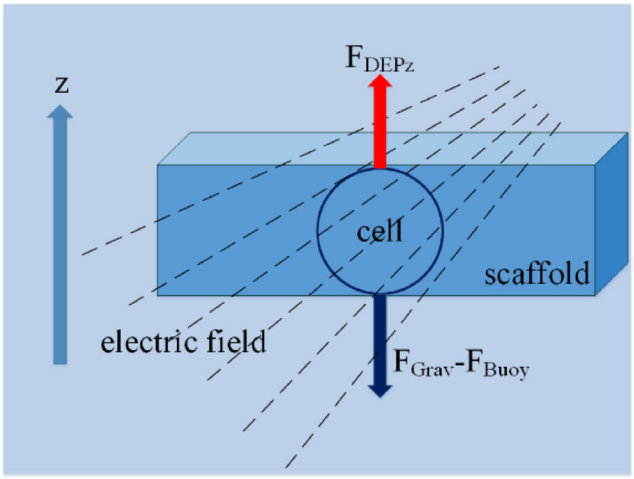

Fig. 6 Force body diagram for an adhered cell

$$F_{Buoy} = \frac{4}{3}\pi R^3 \rho_s g \tag{3.2}$$

$$F_{Drag} = 6\pi\eta R v \tag{3.3}$$

$$m_c\ a = F_{DEP} + F_{Grav} + F_{Buoy} + F_{Drag} \tag{3.4}$$

where R is the cell radius. ρ_c and ρ_s are the densities of the cell and medium, respectively, g is the gravitational acceleration, and η is the viscosity coefficient of the DEP buffer medium. According to Eq. (2.1), the amplitude of the input voltage determines the magnitude of the induced positive DEP force.

As shown in Fig. 6, when the cell adheres to the edge of the scaffold after the movement, the viscous drag of the solution will disappear. The DEP force induced by the manipulation system could be reduced which only needs to hold the cell along the scaffold. The component of the DEP force in the z direction only needs to balance the vertical gravity and buoyancy, preventing the cell from sinking to the bottom of the petri dish, as shown in Eqs. (3.5) and (3.6).

$$F_{DEPz} = 2\pi\varepsilon_s R^3 Re[K(\omega)]\frac{\partial}{\partial z}E_{rms}^2 \tag{3.5}$$

$$F_{DEPz} = F_{Grav} - F_{Buoy} = \frac{4}{3}\pi R^3(\rho_c - \rho_s)g \tag{3.6}$$

In our previous research [27–29], a voltage frequency between 100 and 300 kHz was selected for the manipulation of HFF cells. As we previously observed, an operating frequency at 100 kHz or lower may lead to a relatively low cell-seeding efficiency, and an operating frequency at 300 kHz or higher could reduce the cell viability under the effect of electroporation [30]. In our experiment, to ensure the patterning efficiency and cell viability, the operating frequency was set to 300 kHz.

According to Eq. (2.1), the induced DEP force was determined by the generated electric field within the proposed structure. Moreover, the amplitude of the applied voltage contributes to the strength of the DEP force. To enhance the cell-patterning efficiency, the operating voltage should be optimized. We first examined the voltage in the range from 5 to 20 V. For a high voltage input (20 V), the structure could attract many cells onto the edge of the electrodes, forming a relatively complete cellular configuration, as shown in Fig. 7b. A voltage input at 5 V would generate a much weaker DEP force. As illustrated in Fig. 7a, only nearby cells could be manipulated toward the electrodes. The obtained cellular pattern was non-uniform, which is not suitable for further tissue culturing, as shown in Fig. 7. We also checked the cell viability after the manipulation process. A series of experiments were conducted with different voltage inputs at different operating times, and the results are summarized in Fig. 8a. Although a very integrated cellular pattern could be obtained with a high voltage input, the viability of the cells during the manipulation would be threatened, as illustrated in Fig. 8b, c. Cell viability decreased quickly as the voltage input increased from 5 to 20 V. Therefore, the voltage input should be optimized so that a good manipulated cellular pattern could be obtained as well as high cell viability.

Because an input voltage of 20 V was used, more suspended cells could be attracted. We used this high voltage at the beginning of the manipulation. We reduced the applied voltage as time passed. The alterable input voltage can be given as follows:

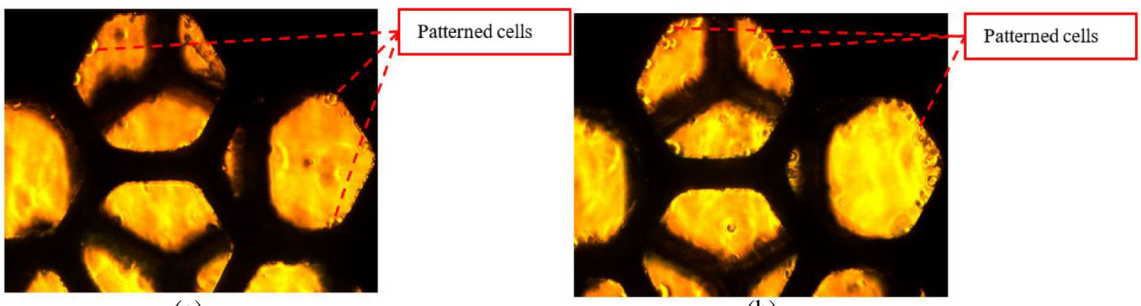

Fig. 7 Cell-patterning experiment at voltages of 5 V (**a**) and 20 V (**b**) in 10 min

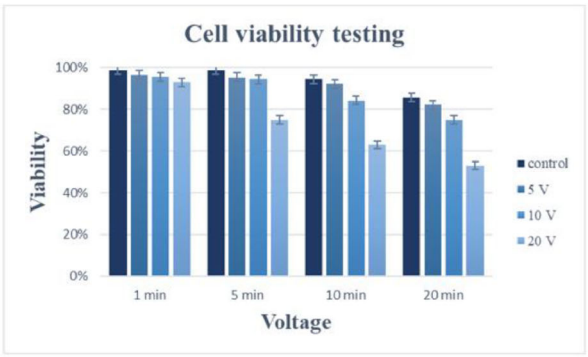

(a)

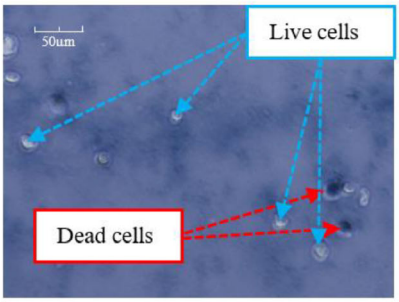

(b)

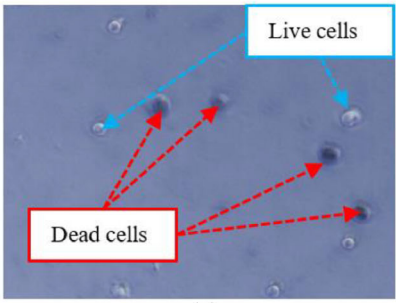

(c)

Fig. 8 Cell viability testing (**a**) with different voltage parameters; under manipulation with 5 V (**b**) input and 20 V input (**c**)

(a)

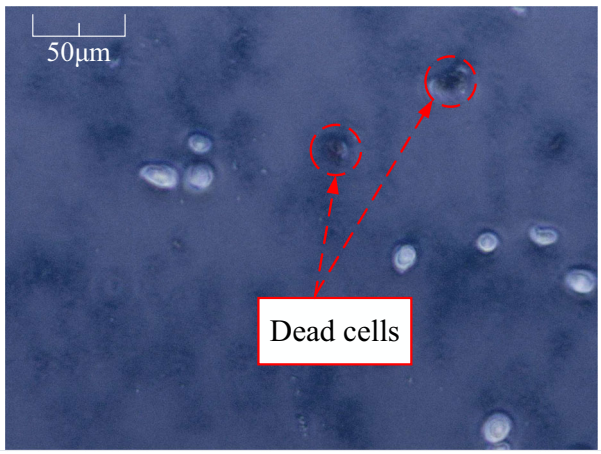

(b)

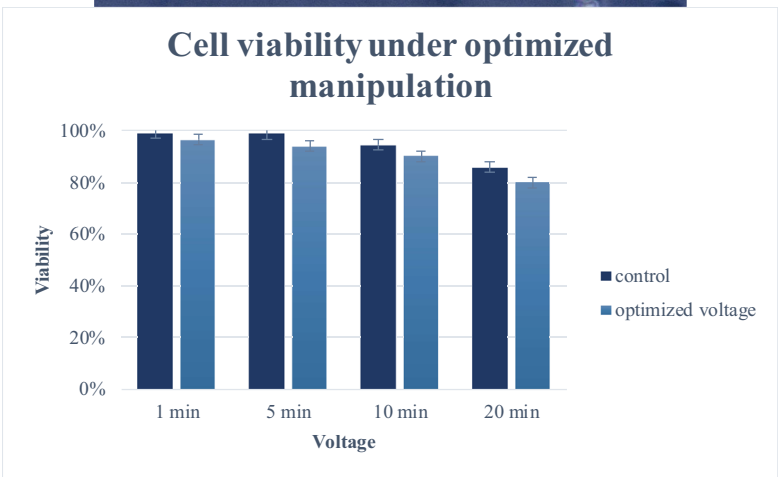

Fig. 9 Cell viability testing (**a**) after the DEP manipulation; Cell viability in different time under the optimized voltage (**b**)

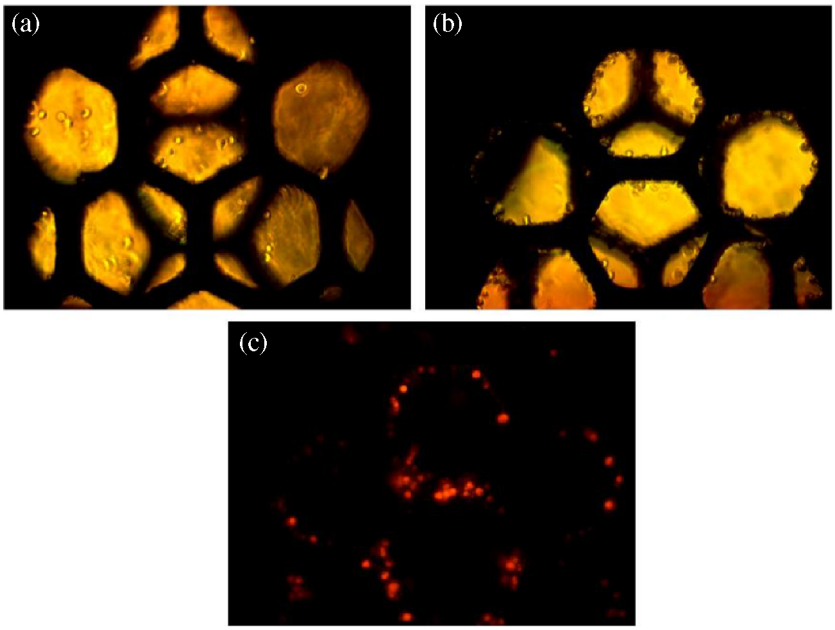

Fig. 10 HFF cells suspended in the space of the structure (**a**); bright-field image (**b**) and fluorescent image (**c**) of the patterned cells

$$U = \begin{cases} 20\ \text{V} & 0\ \text{min} < t < 1\ \text{min} \\ 10\ \text{V} & 1\ \text{min} < t < 5\ \text{min} \\ 5\ \text{V} & 5\ \text{min} < t < 20\ \text{min} \end{cases} \tag{3.7}$$

where U is the output voltage of the function generator and t is the manipulation time. To fix the cells onto the scaffold, the voltage for DEP manipulation was maintained at 5 V for the remaining time of patterning, with which the cells would experience less damage. A cell viability test after DEP manipulation was conducted to examine the effect of the voltage input proposed in Eq. (3.7), as illustrated in Fig. 9. Compared with that shown in Fig. 8c, the number of dead cells was obviously

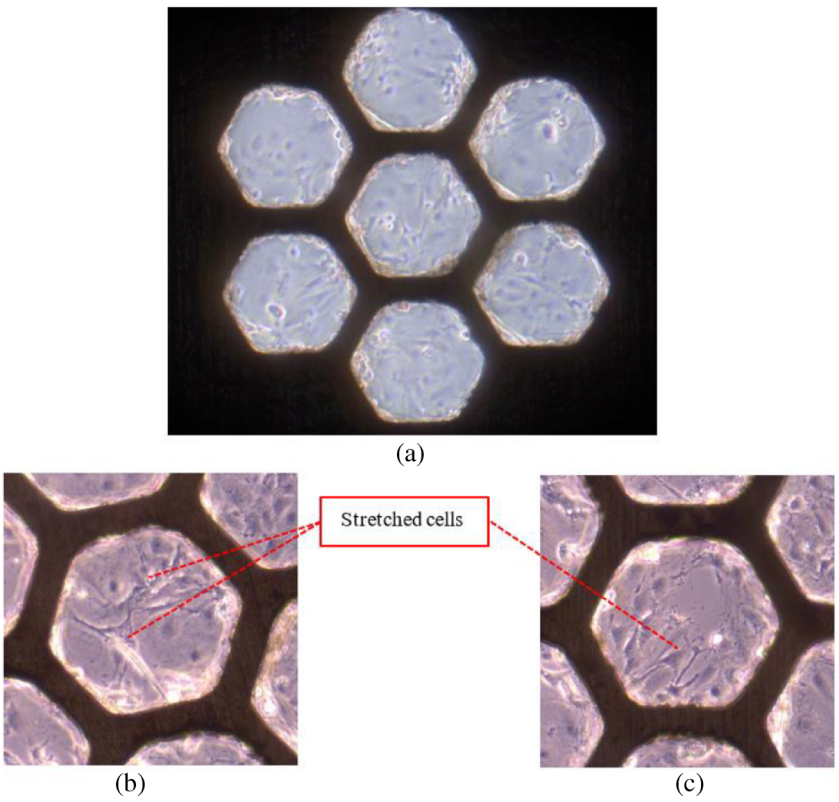

Fig. 11 Micro-images of cells cultured within the structure after 5 days (**a**) and stretched cells (**b**, **c**) in a hexagonal well

reduced, which means that the proposed alterable input voltage is suitable for highly efficient cell manipulation.

3.2 Cell manipulation within the hexagonal structure

As presented in Fig. 2, a fabricated hexagonal structure was used for patterning and culturing of HFF cells. Due to the mechanism of dielectrophoresis, the cells were supposed to be attracted onto the edge of the electrodes. To highlight the cellular pattern during the manipulation process, MitoTracker Red was used to stain the live cells. MitoTracker Red is a red fluorescent dye that stains mitochondria in live cells, which could enhance the contrast of cellular patterns in the captured pictures and videos [31]. Because the HFF cells were cultured in an incubator, we pipetted the culture medium out of the dish and added a preheated MitoTracker Red solution at a concentration of 500 nM at 37 °C. The petri dish was then placed back into the incubator for 30 min. After that, the stained HFF cells were detached from the petri dish and isolated from the medium with a centrifuge. The culture medium was replaced with low conductive medium for further DEP manipulation. The proposed alterable input voltage was utilized for the manipulation of HFF cells, which could ensure a high patterning efficiency.

As shown in Fig. 10a, droplets of the HFF cell solution were pipetted into the wells of the structure. The HFF cells were suspended within the micro-space randomly. When the voltage was supplied, the suspended cells were forced onto the edge of the hexagonal electrodes. As illustrated in Fig. 10b, we focused the microscope on one of the layers and could observe the patterned cells along the edge of the electrodes. Figure 10c shows the fluorescent image of the MitoTracker Red–labeled cells after DEP patterning. The results shown in Fig. 10 indicate that the proposed voltage strategy could realize a high cell-patterning efficiency. Cellular patterns that are more integrated than those shown in Fig. 7 could be obtained. Moreover, because MitoTracker Red is utilized to stain live cells, as observed in Fig. 10b, c, most of the patterned cells were alive, which demonstrates the high cell viability during the manipulation process.

3.3 Cell culturing and stretching within the structure

At the end of the patterning experiment, the input voltage was gradually reduced to zero. Each layer of the thin structure was placed in a 35-mm petri dish, and fresh cell culture medium was slowly added with a syringe pump, which could ensure that the patterned cells would not be washed away. The seeded structure was cultured in the incubator, and the culture medium was changed every 2 days.

After 5 days of culture, a thin layer of structure was observed under a microscope. As presented in Fig. 11a, most of the patterned cells also adhered to the edge of the structure. During the cellular proliferation process of the patterned live cells, the hexagonal space of the provided structure was gradually covered with the stretched cells, as illustrated in Fig. 11b, c.

4 Conclusion

This work proposed a thin layer of structure that could be used to manipulate single cells into certain cellular patterns via dielectrophoresis. This structure could be used for active cell seeding, which enhances cell-patterning efficiency. Because the number of source cells is limited, this method could benefit tissue engineering based on the cell-seeding process. During the experiments, the input voltage was examined and optimized to ensure high cell viability and high cell-patterning efficiency. HFF cells were patterned within the proposed structure through a DEP mechanism. The results show that most of the suspended cells could be attracted onto the edge of the electrodes. This process provides an efficient method for biological cell seeding based on in vitro scaffolds. More experiments were conducted, and the results show that the patterned cells could further proliferate and stretch to fill in the micro-wells of the hexagonal space of the proposed structure. Hence, the proposed hexagonal electrodes and their DEP manipulation mechanism can be used for constructing skin tissue from batches of cells in further tissue engineering.

Funding information This work was supported in part by the Natural Science Foundation of Fujian Province (No. 2019J01869 and No. 2019J05124), the Education Research Project for Young and Middle-aged Teachers of Fujian Province (No. JT180425 and No. JT180426), the Scientific Research Foundation for High Level Talents of Xiamen University of Technology (No. YKJ17012R and No. YKJ17013R), and the Promotion Scientific Research Project Young Teachers (No. XPDKQ18018 and No. XPDKQ18017).

References

1. Lantada D, Andrés AI, Hernán, Pareja Sánchez B (2014) Free-form rapid prototyped porous pdms scaffolds incorporating growth factors promote chondrogenesis. Adv Mater Sci Eng 1:1–10
2. Vashisth P, Nikhil K, Roy P, Pruthi PA, Singh RP, Pruthi V (2016) A novel gellan-PVA nanofibrous scaffold for skin tissue regeneration: fabrication and characterization. Carbohydr Polym 136:851–859
3. Sadeghi-Avalshahr A, Nokhasteh S, Molavi AM, Khorsand-Ghayeni M, Mahdavi-Shahri M (2017) Synthesis and characterization of collagen/PLGA biodegradable skin scaffold fibers. Regen Biomater 4(5):309–314
4. Zhang X, Jia C, Qiao X, Liu T, Sun K (2016) Porous poly(glycerol sebacate) (PGS) elastomer scaffolds for skin tissue engineering. Polym Test 54:118–125
5. Oliveira, Pires Liliana Sofia , F. M. H. F. Vaz , and de Oliveira José Martinho Marques (2018) "Biofabrication of glass scaffolds by 3D printing for tissue engineering." Int J Adv Manuf Technol, 98, 2665–2676

6. Mihailescu M, Paun IA, Zamfirescu M, Luculescu CR, Acasandrei AM, Dinescu M (2016) Laser-assisted fabrication and non-invasive imaging of 3d cell-seeding constructs for bone tissue engineering. J Mater Sci 51(9):4262–4273
7. Xie M, Mills J, Wang Y, Mahmoodi M, Sun D (2016) Automated translational and rotational control of biological cells with a robot-aided optical tweezers manipulation system. IEEE Trans Autom Sci Eng 13(2):543–551
8. Xie M, Li X, Wang Y, Liu Y, Sun D (2017) Saturated PID control for the optical manipulation of biological cells. IEEE Trans Control Syst Technol 99:1–8
9. Xie M, Shakoor A, Shen Y, Mills JK, Sun D (2019) Out-of-plane rotation control of biological cells with a robot-tweezers manipulation system for orientation-based cell surgery. IEEE Trans Biomed Eng 66:199–207
10. Xie M, Shakoor A, Wu C (2018) Manipulation of biological cells using a robot-aided optical tweezers system. Micromachines 9(5): 245
11. Xie M, Mills J, Li X, Wang Y, Sun D (2015) Modelling and Control of Optical Manipulation for Cell Rotation. IEEE International Conference on Robotics and Automation, 956–961.
12. Xu F, Finley TD, Turkaydin M, Sung Y, Gurkan UA, Yavuz AS, Guldiken RO, Demirci U (2011) The assembly of cell-encapsulating microscale hydrogels using acoustic waves. Biomaterials 32(31):7847–7855
13. Ding X, Lin SCS, Kiraly B, Yue H, Li S, Chiang IK, Shi J, Benkovic SJ, Huang TJ (2012) On-chip manipulation of single microparticles, cells, and organisms using surface acoustic waves. Proc Natl Acad Sci 109(28):11105–11109
14. Coquelle E, Bossis G (2006) Mullins effect in elastomers filled with particles aligned by a magnetic field. Int J Solids Struct 43:7659–7672
15. Baghani M, Mohammadi M, Farajpour A (2016) Dynamic and stability analysis of the rotating nanobeam in a non-uniform magnetic field considering the surface energy. Int J Appl Mech 08(04): 1650048
16. Ma W, Li J, Niu F, Ji H, Sun D (2017) Robust control to manipulate a microparticle with electromagnetic coil system. IEEE Trans Ind Electron 64(11):8566–8577
17. Alazzam A, Stiharu I, Bhat R, Meguerditchian AN (2011) Interdigitated comb-like electrodes for continuous separation of malignant cells from blood using dielectrophoresis. Electrophoresis 32(11):1327–1336
18. Ho CT, Lin RZ, Chen RJ, Chin CK, Gong SE, Chang HY, Peng HL, Hsu L, Yew TR, Chang SF, Liu CH (2013) Liver-cell patterning lab chip: mimicking the morphology of liver lobule tissue. Lab Chip 13(18):3578–3587
19. Pohl HA (1978) Dielectrophoresis. Cambridge University Press, Cambridge
20. Hughes MP (2002) Strategies for dielectrophoretic separation in laboratory-on-a-chip systems. Electrophoresis 23(16):2569–2582
21. Pethig R, Huang Y (1995) Dielectrophoretic and electrorotation behaviour of cells: theory and experiment. Bioelectrochemistry of Cells and Tissues, Birkhäuser Basel
22. Dewidar, M. M., Khalil, K. A. and Lim, J. K. (2007) "Processing and mechanical properties of porous 316l stainless steel for biomedical applications," Trans Nonferrous Metals Soc China, 17(3), 0–473, 468
23. Hu J, Zhou Y, and Liu Z (2018) "The friction effect on buckling behavior of cellular structures under axial load," *International Journal of Applied Mechanics*, S1758825118500138
24. Zargar R, Nourmohammadi J, Amoabediny G (2016) Preparation, characterization, and silanization of 3d microporous PDMS structure with properly sized pores for endothelial cell culture. Biotechnol Appl Biochem 63(2):190–199
25. Niepel MS, Almouhanna F, Ekambaram BK, Menzel M, Heilmann A and Groth T (2018) "Cross-linking multilayers of poly-\r, l\r, −lysine and hyaluronic acid: effect on mesenchymal stem cell behavior," Int J Artif Organs, 039139881775259
26. Yoshioka T, Kunimori R, Hisaoka I, Nagasawa H, Kanezashi M, Tsuru T (2019) Molecular dynamics simulation study on the mechanisms of liquid-phase permeation in nanopores. Sep Purif Technol 220:259–267. https://doi.org/10.1016/j.seppur.2019.03.014
27. Chu HK, Huan Z, Mills JK, Yang J, Sun D (2015) Three-dimensional cell manipulation and patterning using dielectrophoresis via a multi-layer scaffold structure. Lab Chip 15(3):920–930
28. Huan Z, Chu HK, Yang J, Sun D (2017) Characterization of a Honeycomb-like Scaffold with Dielectrophoresis-based Patterning for Tissue Engineering. IEEE trans Biomed Eng 64(4):755–764
29. Huan Z, Chu HK, Liu H, Yang J, Sun D (2017) Engineered bone scaffold with dielectrophoresis-based patterning using 3D printing. Biomed Microdevices 19:102
30. Huang C, Liu C, Loo J, Stakenborg T, Lagae L (2014) Single cell viability observation in cell dielectrophoretic trapping on a microchip. Appl Phys Lett 104(1):2216
31. Zhitomirsky B, Farber H, Assaraf YG (2018) Lysotracker and mitotracker red are transport substrates of p-glycoprotein: implications for anticancer drug design evading multidrug resistance. J Cell Mol Med 22(4):2131–2141